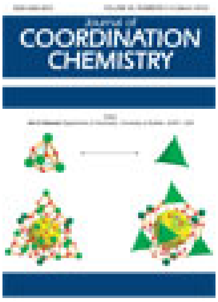

Journal of Coordination Chemistry
Publication details, including instructions for authors and subscription information:
http://www.tandfonline.com/loi/gcoo20

Syntheses, crystal structures, and luminescence of two main-group metal complexes based on 3,4-pyrazoledicarboxylic acid

Li-Dong Wang [a], Feng Tao [a], Mei-Ling Cheng [a], Qi Liu [a b], Wei Han [a], Yu-Juan Wu [a], Dan-Dan Yang [a] & Li-Juan Wang [a]

[a] School of Petrochemical Engineering and Jiangsu Province Key Laboratory of Fine Petro-chemical Technology, Changzhou University, Changzhou 213164, P.R. China

[b] State Key Laboratory of Coordination Chemistry, Nanjing University, Nanjing, Jiangsu 210093, P.R. China

Published online: 27 Feb 2012.

To cite this article: Li-Dong Wang, Feng Tao, Mei-Ling Cheng, Qi Liu, Wei Han, Yu-Juan Wu, Dan-Dan Yang & Li-Juan Wang (2012) Syntheses, crystal structures, and luminescence of two main-group metal complexes based on 3,4-pyrazoledicarboxylic acid, Journal of Coordination Chemistry, 65:6, 923-933, DOI: 10.1080/00958972.2012.663494

To link to this article: http://dx.doi.org/10.1080/00958972.2012.663494

Journal of Coordination Chemistry
Vol. 65, No. 6, 20 March 2012, 923–933

Syntheses, crystal structures, and luminescence of two main-group metal complexes based on 3,4-pyrazoledicarboxylic acid

LI-DONG WANG†, FENG TAO†, MEI-LING CHENG*†, QI LIU*†‡, WEI HAN†, YU-JUAN WU†, DAN-DAN YANG† and LI-JUAN WANG†

†School of Petrochemical Engineering and Jiangsu Province Key Laboratory of Fine Petro-chemical Technology, Changzhou University, Changzhou 213164, P.R. China
‡State Key Laboratory of Coordination Chemistry, Nanjing University, Nanjing, Jiangsu 210093, P.R. China

(*Received 26 November 2011; in final form 2 January 2012*)

Two new metal complexes, $[Pb(H_2pdc)_2(H_2O)]\cdot 2H_2O$ (**1**) and $[Sr_2(H_2pdc)_4(H_2O)_8]\cdot 2H_2O$ (**2**) ($H_3pdc = $ 3,4-pyrazoledicarboxylic acid), have been synthesized and characterized by elemental analysis, IR spectra, and single-crystal X-ray diffraction. In **1**, the geometry of Pb(II) is hemidirected and the $6s^2$ lone electron pair on Pb(II) is stereochemically active, resulting in the formation of a secondary Pb$\cdots$O bond. The weak Pb$\cdots$O interactions, π–π stacking, and hydrogen-bonding interactions construct **1** into a 3-D framework with 1-D channels. Complex **2** is a dinuclear structure, which is further assembled to a 3-D supramolecular network through intermolecular hydrogen bonds and π–π stacking. Three coordination modes of 3,4-pyrazoledicarboxylic acid were observed. The thermal and photoluminescent properties of **1** and **2** in the solid state have also been investigated.

Keywords: Lead(II); Strontium(II); 3,4-pyrazoledicarboxylic acid; Crystal structure; Photoluminescence

1. Introduction

Design and synthesis of supramolecular metal–organic architectures with channels constructed by coordination bonds and/or other weak cooperative interactions such as hydrogen-bonding and π–π stacking is a rapidly growing research area owing to intriguing structural features and potential application in catalysis, separations, gas storage, and optoelectronics [1–8]. Assembly of these supramolecular complexes mainly depends on coordination geometry of metal ions and the chemical structure and property of ligands. One synthetic strategy used to construct 3-D supramolecular architectures with channels involves making a combination of bridging multidentate ligands with suitable metal ions. Heterocyclic carboxylic acids, such as pyridinecarboxylic acid [9–11], pyrazolecarboxylic acid [12–15], and imidazolecarboxylic acid [16–19], as multidentate ligands have been investigated due to their multi-coordination

*Corresponding authors. Email: chengmeiling01@163.com; liuqi62@163.com

Journal of Coordination Chemistry
ISSN 0095-8972 print/ISSN 1029-0389 online © 2012 Taylor & Francis
http://dx.doi.org/10.1080/00958972.2012.663494

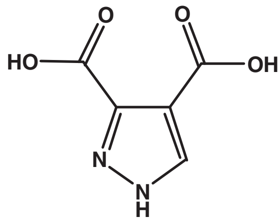

Scheme 1. Molecular structure of H_3pdc.

modes by the N and O donors on the heterocyclic rings and the carboxyl groups. As proton donors and acceptors, the carboxylic oxygen atoms and nitrogen atoms in heterocyclic carboxylic acids can not only coordinate as monodentate or multidentate ligands, but also provide intermolecular hydrogen bonds for assembling the complex into high-dimensional supramolecular networks. For example, 3,5-pyrazoledicarboxylic acid, a rigid heterocyclic carboxylic acid, has been widely used to synthesize various supramolecular metal–organic architectures containing transition, lanthanide, and alkaline-earth metals [20–22]. Similar to 3,5-pyrazoledicarboxylic acid, 3,4-pyrazoledicarboxylic acid (H_3pdc) (scheme 1) has potential coordination sites involving both nitrogen atoms of the pyrazole ring and carboxylate oxygen atoms. H_3pdc can be partially or fully deprotonated to generate H_2pdc^-, $Hpdc^{2-}$, and pdc^{3-} at different pH values, which is useful to synthesize new complexes. However, to the best of our knowledge, studies of complexes using 3,4-pyrazoledicarboxylic acid ligand have not been explored. In order to extend the investigation in this field, we synthesized $[Pb(H_2pdc)_2(H_2O)] \cdot 2H_2O$ (**1**) and $[Sr_2(H_2pdc)_4(H_2O)_8] \cdot 2H_2O$ (**2**). Herein, we report the syntheses, crystal structures, and luminescent properties of the complexes.

2. Experimental

2.1. *Materials*

3,4-Pyrazoledicarboxylic acid (H_3pdc) was synthesized according to literature methods [23]. All reagents and solvents employed were commercially available and used as received.

2.2. *Physical measurements*

Elemental analyses (C, H, and N) were performed on a Perkin-Elmer 2400 Series II element analyzer. FTIR spectra were recorded on a Nicolet 460 spectrophotometer as KBr pellets. Luminescence spectra of solid samples were recorded on a Varian Cary Eclipse spectrometer. Thermogravimetric analysis experiments were carried out on a Dupont thermal analyzer from room temperature to 790°C under N_2 at a heating rate of 10°C min^{-1}. Single-crystal X-ray diffraction measurements of the two compounds were carried out with a Bruker Apex II CCD diffractometer at 291(2) K and 293(2) K, respectively.

2.3. *Synthesis of [Pb(H$_2$pdc)$_2$(H$_2$O)]·2H$_2$O (1)*

H_3pdc (0.10 mmol, 0.0156 g) and $Pb(NO_3)_2$ (0.10 mmol, 0.0330 g) were added to a mixed solvent of 6 mL anhydrous ethanol and 4 mL deionized water and stirred for 1 h. The resulting colorless solution was allowed to stand at ambient temperature for 2 weeks to afford colorless crystals of **1** in 65.31% yield (based on Pb). Anal. Calcd for $C_{10}H_{12}PbN_4O_{11}$ (%): C, 27.38; H, 2.68; N, 12.71. Found: C, 27.22; H, 2.62; N, 12.69. IR data (cm^{-1}, KBr pellet): 3460 (s), 3210 (s), 3135 (s), 1693 (s), 1544 (s), 1510 (vs), 1383 (s), 1337 (s), 1110 (s), 948 (s), 765 (m).

2.4. *Synthesis of [Sr$_2$(H$_2$pdc)$_4$(H$_2$O)$_8$]·2H$_2$O (2)*

Complex **2** was synthesized by a procedure similar to that of **1**, except using $SrCl_2 \cdot 6H_2O$ (0.10 mmol, 0.0266 g) instead of $Pb(NO_3)_2$. A colorless solution was allowed to stand at ambient temperature for 6 days, yielding colorless crystals of **2** in 55.32% yield (based on Sr). Anal. Calcd for $C_{20}H_{32}Sr_2N_8O_{26}$ (%): C, 27.38; H, 2.68; N, 12.71. Found: C, 27.22; H, 2.62; N, 12.69. IR data (cm^{-1}, KBr pellet): 3537 (s), 3433 (s), 3191 (s), 3106 (s), 1693 (s), 1540 (vs), 1434 (s), 1390 (s), 1356 (s), 1247 (m), 1107 (m), 1082 (m), 1033 (m), 952 (m), 851 (m), 775 (s).

2.5. *X-ray crystallography*

Single-crystal X-ray diffraction measurements of **1** and **2** were carried out with a Bruker Smart Apex CCD diffractometer at 291(2) K and 293(2) K, respectively. Intensities of reflections were measured using graphite-monochromated Mo-Kα radiation ($\lambda = 0.71073$ Å) with the ψ–ω scans mode from $1.96 < \theta < 26.00°$ (**1**) and $2.35 < \theta < 24.99°$ (**2**). The structure was solved by direct methods using SHELXTL-97 [24] and refined by full-matrix least-squares on F^2 with the SHELXTL-97 [24] program package. Anisotropic thermal factors were assigned to all the non-hydrogen atoms. Hydrogen atoms were included in calculated positions and refined with isotropic thermal parameters riding on the parent atoms. Crystallographic data and experimental details for structural analyses are summarized in table 1.

3. Results and discussion

3.1. *Crystal structure of 1*

X-ray crystal structure analysis reveals that **1** crystallizes in the monoclinic space group $P2_1/c$. The asymmetric unit of **1** contains one Pb(II), two H_2pdc^-, and three water molecules. As illustrated in figure 1, two crystallographically equivalent Pb(II) ions are bridged by two H_2pdc^- anions with N,O-chelating and μ_2-O-bridging to form a four-membered ring with Pb(1)–Pb(1 A) distance of 4.219(4) Å. The coordination sphere of Pb(II) is defined by three carboxylic oxygen atoms (O(1), O(5), O(1 A)), two pyrazole nitrogen atoms (N(1), N(3)) from three individual H_2pdc^- ligands, and one oxygen (O(9)) from water molecule, leading to a distorted pentagonal pyramidal geometry. The geometry of Pb(II) ion is hemidirected according to the literature [25, 26], and there is a

Table 1. The crystal data, experimental conditions, and structure refinement parameters of **1** and **2**.

Compound	**1**	**2**
Empirical formula	$C_{10}H_{12}PbN_4O_{11}$	$C_{20}H_{32}Sr_2N_8O_{26}$
Formula weight	571.43	975.78
Color, shape	Colorless, prism	Colorless, prism
Temperature (K)	291(2)	293(2)
Wavelength (nm)	0.071073	0.071073
Crystal system	Monoclinic	Triclinic
Space group	$P2_1/c$	$P\bar{1}$
Unit cell dimensions (Å,°)		
a	6.9500(5)	7.2476(8)
b	14.5969(11)	7.2772(4)
c	16.1734(9)	17.830(2)
α	90.00	91.992(2)
β	114.295(2)	101.404(2)
γ	90.00	111.192(2)
Volume (Å^3), Z	1495.46(18), 4	853.66(16), 1
Calculated density (g cm^{-3})	2.538	1.898
Absorption coefficient (Mo-Kα) (mm^{-1})	0.8413	0.8411
$F(000)$	1080	492
Crystal size (mm^3)	$0.24 \times 0.22 \times 0.18$	$0.30 \times 0.24 \times 0.20$
θ range for data collection (°)	1.96–26.00	2.35–24.99
Index ranges (h, k, l)	$-8 \leq h \leq 8$; $-17 \leq k \leq 12$; $-19 \leq l \leq 19$	$-8 \leq h \leq 8$; $-8 \leq k \leq 8$; $-21 \leq l \leq 19$
Independent reflections (R_{int})	2921	2977
Refinement method	Full-matrix least-squares on F^2	Full-matrix least-squares on F^2
Data/restraints/parameters	2921/1/237	2977/4/255
Goodness-of-fit on F^2	1.011	0.892
R_1, wR_2 [$I > 2\sigma(I)$]	0.0265, 0.0617	0.0284, 0.0871
R_1, wR_2 (all data)	0.0370, 0.0656	0.0302, 0.0884
Largest difference peak and hole (e Å^{-3})	0.755 and –0.942	0.456 and –0.455

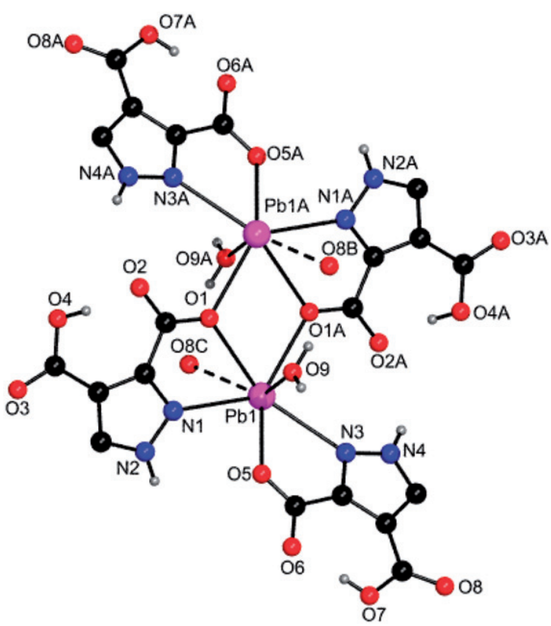

Figure 1. The coordination environment of Pb(II) in **1**. Broken lines represent the secondary bonds. Symmetry codes: A: $2 - x$, $2 - y$, $1 - z$; B: $2 - x$, $0.5 + y$, $0.5 + z$; C: x, $1.5 - y$, $0.5 + z$.

Table 2. Selected bond distances (Å) and angles (°) for **1**.

Bond distances			
Pb(1)–N(1 A)	2.618(5)	Pb(1)–N(3)	2.745(5)
Pb(1)–O(5)	2.515(4)	Pb(1)–O(1)	2.622(4)
Pb(1)–O(9)	2.419(4)	Pb(1 A)–O(1)	2.696(4)
Pb(1) ··· O(8)	2.970(5)		
Bond angles			
N(3)–Pb(1)–O(5)	61.95(13)	N(1 A)–Pb(1)–O(5)	70.81(14)
N(1 A)–Pb(1)–O(1 A)	60.34(14)	O(1 A)–Pb(1)–O(1 A)	67.49(14)
N(3)–Pb(1)–O(1)	94.54(13)	O(5)–Pb(1)–O(1 A)	117.47(12)
O(9)–Pb(1)–O(1)	70.43(13)	O(5)–Pb(1)–O(1)	140.57(13)

Symmetry code: A: 2 − *x*, 2 − *y*, 1 − *z*.

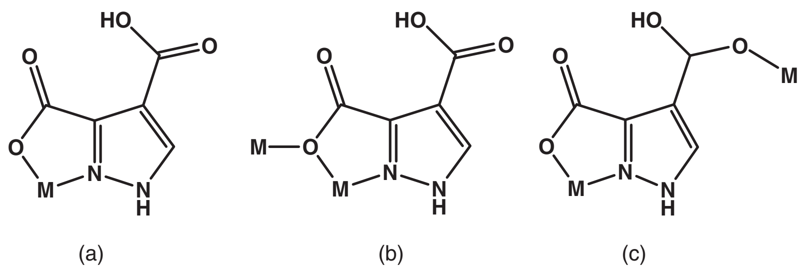

Scheme 2. Different coordination modes of H_3pdc in **1** and **2**.

clear identifiable gap in the coordination sphere of Pb(II), suggesting that Pb(II) contains a stereochemically active $6s^2$ lone electron pair [27]. Recently, "primary bond" and "secondary bond" have been used to describe the environment of Pb(II) [27]. Six coordination bonds termed as primary bonds are observed in **1**. Pb–N and Pb–O bond lengths lie in the range of 2.618(5)–2.745(5) Å and 2.419(4)–2.696(4) Å, respectively, comparable to those reported for other Pb(II) complexes [28, 29]. However, the secondary bond of Pb(II) with carboxylic oxygen atoms of an adjacent molecule Pb(1) ··· O(8) with a distance of 2.970(5) Å (dashed lines in figure 1) is longer than the sum of the ionic radii but significantly shorter than the sum of the van der Waals radii (3.54 Å) [30], which can be explained by the presence of an active lone electron pair in the proximity of the oxygen. If the Pb(1) ··· O(8) bond is taken into account, then the geometry around lead(II) ion can be described as a seven-coordinate pentagonal bipyramid. The bond angles around Pb(II) are in the range of 60.34(14)° and 140.57(13)° (table 2). H_2pdc^- in **1** adopts two coordination modes (scheme 2a and b). In one H_2pdc^- coordinates to Pb(II) in a N,O-chelating fashion (with a five-membered chelate ring) through the carboxylate oxygen atom and its adjacent nitrogen atom in the pyrazole ring (scheme 2a), the other coordinates to two Pb(II) ions through N,O-chelating and μ_2-O-bridging modes (scheme 2b). Adjacent $[Pb(H_2pdc)_2(H_2O)]$ molecules are stacked face-to-face with a separation of 3.434(4) Å between the centroids of the two pyrazolyl rings, indicating the existence of significant π–π interactions (figure 2). Therefore, the discrete dinuclear structure is further cross-linked *via* the weak Pb ··· O interactions, intermolecular hydrogen bonds (O(9)–H(9X) ··· $O(3)^{i}$, O(9)–H(9Y) ··· $O(8)^{ii}$), and π–π stacking to generate a 2-D grid (figure 2). These 2-D

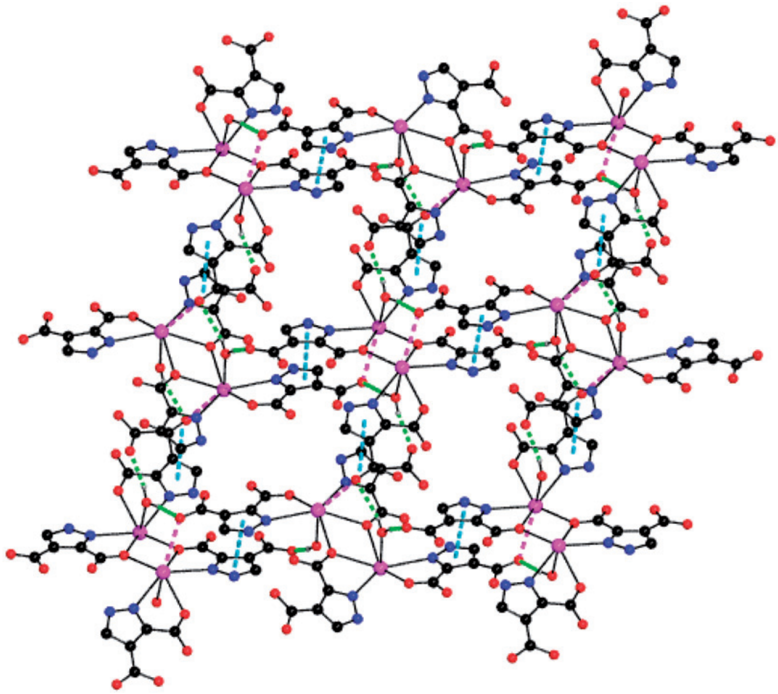

Figure 2. The 2-D layer network motif of **1** constructed by the weak Pb···O interactions, π–π stacking, and hydrogen-bonding interactions. Only hydrogen atoms involved in hydrogen bonds are shown.

layers are packed through O(11)–H(11X)···O(4)^{v}, O(10)–H(10Y)···O(6)^{iv}, N(2)–H(2)···O(11)^{vii}, and N(4)–H(4)···O(10)^{viii} hydrogen bonds to construct a stable 3-D supramolecular architecture (figure 3). The data of the intermolecular hydrogen bonds are listed in table 3. One of the most notable structural features of **1** is that there are many 1-D channels with dimensions 13.671 × 7.141 Å in its 3-D networks along the *b*-axis, as shown in figure 3. The results indicate that weak non-covalent interactions are important in the formation of the final supramolecular structure of **1**.

3.2. *Crystal structure of 2*

X-ray crystal structure analysis reveals that **2** crystallizes in the triclinic space group *P*ı. The asymmetric unit of **2** contains one Sr(II), two H_2pdc^-, and five water molecules. As shown in figure 4, quite differently from the coordination environment in **1**, Sr(1) and Sr(1 A) are linked to form a binuclear unit by two individual H_2pdc^- ligands *via* monodentate and N,O-chelating bidentate modes (scheme 2c). The distance between two Sr(II) ions (Sr(1)–Sr(1A) = 8.443(9) Å) is longer than that between two Pb(II) ions in **1**; the different distance may be attributed to the different coordination modes of H_2pdc^-. The Sr(II) is nine-coordinate, surrounded by one nitrogen atom (N(3)) and one oxygen atom (O(5)) from a H_2pdc^- in a chelating fashion (scheme 2a), two carboxylic oxygen atoms (O(1), O(3 A)) and one pyrazole nitrogen atom (N1) from two

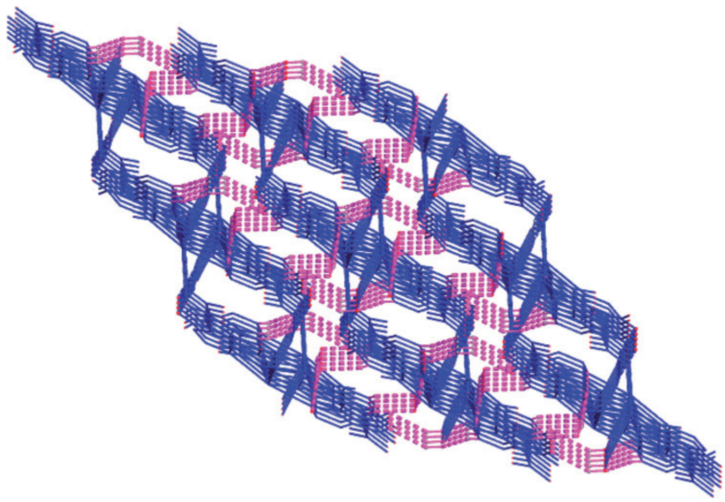

Figure 3. The 3-D network of **1** constructed by hydrogen-bonding with 1-D channels along the *b*-axis (broken lines represent hydrogen-bonding interactions).

Table 3. Hydrogen-bond distances and angles for **1**.

D–H···A	D–H (Å)	H···A (Å)	D···A (Å)	D–H···A (°)
O(9)–H(9X)···O(3)^{i}	0.82	2.01	2.819(6)	168
O(9)–H(9Y)···O(8)^{ii}	0.82	2.31	3.090(5)	158
O(9)–H(9Y)···O(7)^{ii}	0.82	2.51	3.206(6)	143
O(10)–H(10X)···N(2)^{iii}	0.85	2.44	3.112(6)	137
O(10)–H(10Y)···O(6)^{iv}	0.85	2.35	3.191(5)	168
O(10)–H(10Y)···O(5)^{iv}	0.85	2.42	2.986(6)	125
O(11)–H(11X)···O(4)^{v}	0.82	2.17	2.893(5)	147
O(11)–H(11Y)···O(6)^{vi}	0.82	2.12	2.845(5)	148
N(2)–H(2)···O(11)^{vii}	0.86	1.87	2.714(6)	166
N(4)–H(4)···O(10)^{viii}	0.86	2.15	2.844(6)	137

Symmetry code: ^{i} 2 − *x*, −1/2 + *y*, 1/2 − *z*; ^{ii} 2 − *x*, 1/2 + *y*, 1/2 − *z*; ^{iii} *x*, −1 + *y*, *z*; ^{iv} 2 − *x*, 1 − *y*, 1 − *z*; ^{v} *x*, 3/2 − *y*, 1/2 + *z*; ^{vi} −1 + *x*, *y*, *z*; ^{vii} 1 + *x*, 1 + *y*, *z*; ^{viii} 1 − *x*, 1/2 + *y*, 1/2 − *z*.

H_2pdc^- ligands; the remaining positions are occupied by four water molecules (O(9), O(10), O(11), O(12)), forming a distorted tricapped trigonal geometry, which is close to other Sr(II) coordination polymers reported [31]. The Sr–N bond lengths are 2.726(2)–2.731(2) Å and Sr–O bond lengths vary from 2.619(2) to 2.717(2) Å (table 4), close to the values in other Sr(II) complexes [32, 33]. The bond angles around Sr(II) are 59.27(6)° and 149.39(7)°. Complex **2** contains multiple hydrogen bonds between coordinated water molecules and adjacent carboxyl oxygen atoms. As shown in table 5, hydrogen-bond lengths and angles of O–H···O are 2.850(3)–3.123(3) Å and 147–170°, respectively. The independent components $[Sr_2(H_2pdc)_2(Hpdc)_2(H_2O)_8]$ are linked by O(9)–H(9X)···O(5)^{i} and O(9)–H(9Y)···O(8)^{ii} hydrogen bonds to form 2-D nets with $R_2^2(18)$ ring pattern. These 2-D hydrogen-bonded layers are packed along the *a*-axis through O(10)–H(10X)···O(1)^{iii}, O(11)–H(11Y)···O(4)^{v}, O(12)–H(12X)···O(13), and O(13)–H(13X)···O(3)^{v} hydrogen bonds to construct a 3-D supramolecular

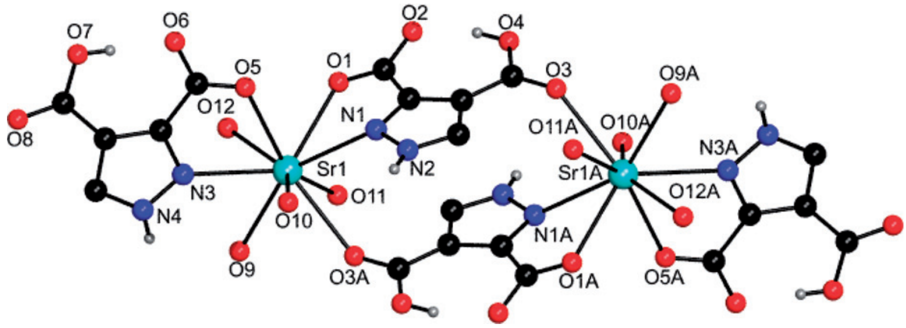

Figure 4. The coordination environment of Sr(II) in **2**. Symmetry codes: A: $-x$, $-y$, $-z$.

Table 4. Selected bond distances (Å) and angles (°) for **2**.

Sr(1)–N(1)	2.726(2)	Sr(1)–O(1)	2.717(2)
Sr(1)–N(3)	2.731(2)	Sr(1)–O(3)	2.715(2)
Sr(1)–O(9)	2.619(2)	Sr(1)–O(5)	2.670(2)
Sr(1)–O(11)	2.629(2)	Sr(1)–O(12)	2.625(2)
N(1)–Sr(1)–N(3)	130.07(7)	N(3)–Sr(1)–O(1)	125.83(7)
N(3)–Sr(1)–O(3 A)	121.56(7)	N(3)–Sr(1)–O(5)	60.11(6)
N(3)–Sr(1)–O(12)	72.08(7)	N(3)–Sr(1)–O(11)	134.40(7)
N(3)–Sr(1)–O(10)	72.84(7)	N(3)–Sr(1)–O(9)	71.05(8)
N(1)–Sr(1)–O(1)	59.27(6)	N(1)–Sr(1)–O(3 A)	75.38(7)
N(1)–Sr(1)–O(11)	95.37(7)	N(1)–Sr(1)–O(10)	70.83(7)
N(1)–Sr(1)–O(9)	149.39(7)	N(1)–Sr(1)–O(5)	78.65(6)
N(1)–Sr(1)–O(12)	129.67(7)	O(1)–Sr(1)–O(3 A)	112.45(6)
O(1)–Sr(1)–O(5)	75.16(7)	O(1)–Sr(1)–O(12)	71.40(6)
O(1)–Sr(1)–O(11)	70.00(7)	O(1)–Sr(1)–O(10)	125.98(7)
O(1)–Sr(1)–O(9)	131.71(7)	O(5)–Sr(1)–O(3 A)	142.53(7)
O(9)–Sr(1)–O(10)	101.72(8)	O(9)–Sr(1)–O(11)	69.62(8)
O(10)–Sr(1)–O(11)	137.42(7)	O(9)–Sr(1)–O(12)	73.88(7)
O(11)–Sr(1)–O(12)	75.63(7)	O(10)–Sr(1)–O(5)	76.13(7)

Symmetry code: A: $-x$, $-y$, $-z$.

Table 5. Hydrogen-bond distances and angles for **2**.

D–H···A	D–H (Å)	H···A (Å)	D···A (Å)	D–H···A (°)
O(9)–H(9X)···O(5)^{i}	0.77	2.15	2.913(3)	169
O(9)–H(9Y)···O(8)^{ii}	0.85	2.10	2.857(4)	147
O(10)–H(10X)···O(1)^{iii}	0.82	2.04	2.850(3)	170
O(10)–H(10Y)···O(8)^{iv}	0.82	2.05	2.842(3)	165
O(11)–H(11Y)···O(4)^{v}	0.82	2.34	3.123(3)	159
O(12)–H(12X)···O(13)	0.82	1.98	2.786(3)	165
O(12)–H(12Y)···O(7)^{vi}	0.82	2.14	2.889(3)	151
O(13)–H(13X)···O(3)^{v}	0.82	2.08	2.880(3)	165
O(13)–H(13Y)···O(5)^{vii}	0.82	2.27	3.003(3)	149

Symmetry code: ^{i} x, $1+y$, z; ^{ii} $1-x$, $1-y$, $1-z$; ^{iii} $-1+x$, y, z; ^{iv} $-x$, $-y$, $1-z$; ^{v} $1-x$, $-y$, $-z$; ^{vi} $1-x$, $-y$, $1-z$; ^{vii} $1+x$, $1+y$, z.

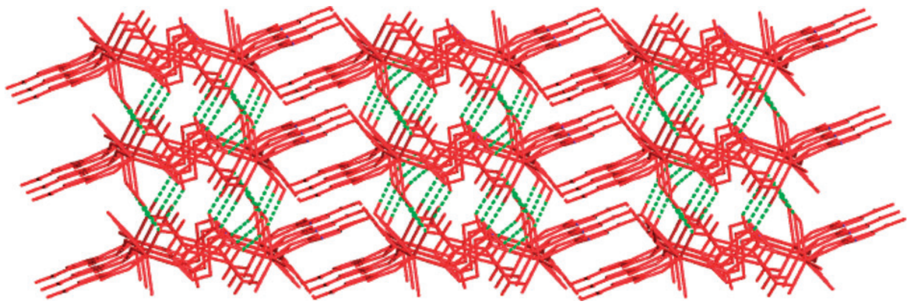

Figure 5. The 3-D network of **2** along the *a*-axis linked by hydrogen bonds (broken lines represent hydrogen-bonding interactions).

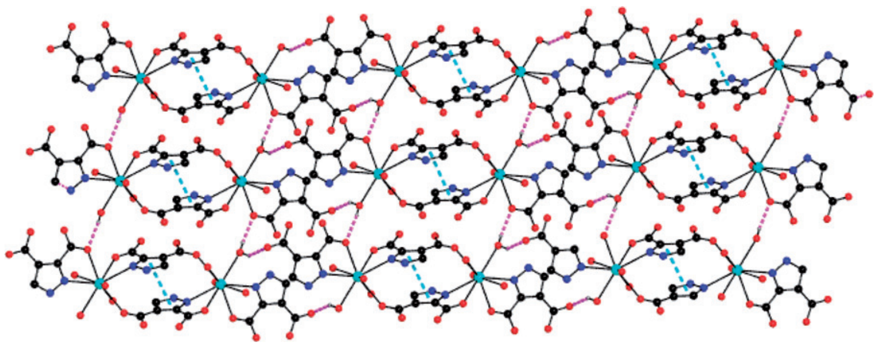

Figure 6. The 2-D layer network of **2** *via* hydrogen-bonding and π–π stacking interactions. Only hydrogen atoms involved in hydrogen bonds are shown.

architecture (figure 5). Adjacent $[Sr_2(H_2pdc)_2(Hpdc)_2(H_2O)_8]$ molecules are stacked face-to-face with a separation of 3.355(16) Å between the centroids of the two pyrazolyl rings, indicating intermolecular π–π interactions, which also play a significant role in the formation of the final supramolecular structure of **2** (figure 6). The structural difference of **1** and **2** is mainly related to the radius and electronic configuration of Pb(II) and Sr(II). Although Pb(II) ion in **1** has a stereochemically active lone electron pair, its radius is smaller than that of Sr(II), resulting in Pb(II) ion only having seven-coordinate geometry while Sr(II) is nine-coordinate.

3.3. *Thermal analysis*

In order to examine the thermal stabilities of **1** and **2**, thermal gravimetric (TG) analyses were carried out from 20°C to 790°C under nitrogen, as shown in "Supplementary material." For **1**, the TG analysis shows that weight loss begins at 238°C and all water molecules are lost from 238°C to 287°C (Calcd 24.08%; found, 23.96%). One H_3pdc decomposed gradually from 280°C to 510°C (Calcd 36.12%; found, 37.11%). The final experimental residual percentage (38.95%) is consistent with the calculated value of 37.81%, which indicates the final product is PbO. Complex **1** begins to decompose at

238°C, showing it has high thermal stability and its microporous framework is maintained up to 238°C, which is mainly attributable to the strong hydrogen-bonding interactions and the secondary bond Pb ... O interactions. For **2**, the initial weight loss of 19.90% (Calcd 18.56%) occurs from 89°C to 153°C, corresponding to loss of eight water molecules. Above 153°C, the complex is destroyed gradually. The final residue of 19.03% is in agreement with the percentage of SrO (Calcd 20.19%).

3.4. *Luminescent properties*

The solid-state luminescences of free H_3pdc, **1**, and **2** were investigated at room temperature (Supplementary material). H_3pdc, **1**, and **2** exhibit luminescence with emission maxima at 440, 421, and 421 nm upon excitation at 330, 370, and 370 nm, respectively. The emissions of free ligand may be attributed to the $\pi \rightarrow \pi^*$ transitions. Although the maximum emission wavelengths of **1** and **2** undergo a blue-shift, the emission bands for **1** and **2** are very similar to that of the free ligand in terms of position and band shape. The significant blue-shift of 19 nm should be attributed to the ligand-to-metal charge transfer [34–36]. Moreover, the intensity increase of the luminescence for **1** and **2** may be attributed to chelation of the ligand to metal, which increases the rigidity of H_2pdc^- and reduces the non-radiative relaxation.

4. Conclusion

Two new complexes, $[Pb(H_2pdc)_2(H_2O)] \cdot 2H_2O$ (**1**) and $[Sr_2(H_2pdc)_4(H_2O)_8] \cdot 2H_2O$ (**2**), have been isolated by reaction of corresponding metal salts with H_3pdc. In **1**, the $6s^2$ lone electron pair on Pb(II) is stereochemically active, and the discrete dinuclear units $[Pb_2(H_2pdc)_4(H_2O)_2]$ are linked *via* weak Pb $\cdots$ O interactions, π–π stacking and hydrogen-bonding to generate a 2-D grid. These 2-D layers are further linked to form a 3-D supramolecular network with 1-D channels. The microporous framework of **1** is stable to 238°C. Complex **2** is a dinuclear structure, further assembled to 3-D supramolecular networks through intermolecular hydrogen bonds. Weak non-covalent interactions play an important role in the formation of the final supramolecular structures of **1** and **2**. Moreover, three new coordination modes of H_3pdc were observed in **1** and **2**. Two complexes display strong purple fluorescence in the solid state at room temperature, indicating they may be good candidates for photoactive materials.

Supplementary material

CCDC 849703 and 849704 contain the supplementary crystallographic data for **1** and **2**. These data can be obtained free of charge at www.ccdc.cam.ac.uk/conts/retrieving.html, or from the Cambridge Crystallographic Data Center, 12 Union Road, Cambridge CB2 1EZ, UK; Fax: (internet)+44-1223/336-033; E-mail: deposit@ccdc.cam.ac.uk.

Acknowledgments

The authors thank the Natural Science Foundation of China (Nos 20671045, 20971060, and 21101018), the Natural Science Foundation of State Key Laboratory of Coordination Chemistry, and the International Science and Technology Cooperation Project of Changzhou city (CZ20110023) for the financial support.

References

[1] D. Uraguchi, Y. Ueki, T. Ooi. *Science*, **326**, 120 (2009).
[2] M.D. Allendorf, C.A. Bauer, R.K. Bhakta, R.J.T. Houk. *Chem. Soc. Rev.*, **38**, 1330 (2009).
[3] L. Pan, M.B. Sander, X.Y. Huang, J. Li, M. Smith, E. Bittner, B. Bockrath, J.K. Johnson. *J. Am. Chem. Soc.*, **126**, 1308 (2004).
[4] B. Wang, A.P. Côté, H. Furukawa, M. O'Keeffe, O.M. Yaghi. *Nature*, **453**, 207 (2008).
[5] J.R. Li, R.J. Kuppler, H.C. Zhou. *Chem. Soc. Rev.*, **38**, 1477 (2009).
[6] S.Q. Ma, H.C. Zhou. *Chem. Commun.*, **46**, 44 (2010).
[7] K.T. Holman, A.M. Pivovar, M.D. Ward. *Science*, **294**, 1907 (2001).
[8] T. Uemura, N. Yanai, S. Kitagawa. *Chem. Soc. Rev.*, **38**, 1228 (2009).
[9] S.Y. Niu, J. Jin, Y.X. Chi. *Inorg. Chim. Acta*, **362**, 3821 (2009).
[10] Y.C. Liang, R. Cao, W.P. Su, M.C. Hong. *Angew. Chem., Int. Ed.*, **39**, 3304 (2000).
[11] Y.H. Zhao, H.B. Xu, K.Z. Shao, Y. Xing, Z.M. Su, J.F. Ma. *Cryst. Growth Des.*, **3**, 513 (2007).
[12] S.Y. Zhang, Y.H. Li, W. Li. *Inorg. Chim. Acta*, **362**, 2247 (2009).
[13] X.H. Zhou, X.D. Du, G.N. Li, J.L. Zuo, X.Z. You. *Cryst. Growth Des.*, **9**, 4487 (2009).
[14] X. Feng, L.Y. Wang, J.S. Zhao, B. Liu, J.G. Wang, X.G. Shi. *Inorg. Chim. Acta*, **362**, 5127 (2009).
[15] Y.G. Sun, M.Y. Guo, G. Xiong, F. Ding, L. Wang, B. Jiang, M.C. Zhu, E.J. Gao, F. Verpoort. *J. Coord. Chem.*, **63**, 4188 (2010).
[16] W.G. Lu, L. Jiang, X.L Feng, T.B. Lu. *Inorg. Chem.*, **48**, 6997 (2009).
[17] J.D. Lin, J.W. Cheng, S.W. Du. *Cryst. Growth Des.*, **8**, 3345 (2008).
[18] R.Q. Fang, X.M. Zhang. *Inorg. Chem.*, **45**, 4801 (2006).
[19] W.G. Lu, L. Jiang, X.L. Feng, T.B. Lu. *Cryst. Growth Des.*, **6**, 564 (2006).
[20] J. Xia, B. Zhao, H.S Wang. *Inorg. Chem.*, **46**, 3450 (2007).
[21] L. Pan, T. Frydel, M.B. Sander, X. Huang, J. Li. *Inorg. Chem.*, **40**, 1271 (2001).
[22] C.X. An, Y.C. Lu, Z.F. Shang. *Inorg. Chim. Acta*, **361**, 2721 (2008).
[23] R.G. Jones. *J. Am. Chem. Soc.*, **73**, 3684 (1951).
[24] G.M. Sheldrick. *SHELXTL-97, Program for X-ray Crystal Structure Determination*, University of Göttingen, Germany (1997).
[25] H. Sadeghzadeh, A.M. Veysel, T. Yilmaz, O. Büyükgüngör. *J. Coord. Chem.*, **63**, 3423 (2010).
[26] X.X. Xu, X.X. Liu, X.G. Sang, E.B. Wang. *J. Coord. Chem.*, **63**, 3060 (2010).
[27] X.H. Miao, L.G. Zhu. *Inorg. Chim. Acta*, **361**, 2828 (2008).
[28] Y.L. Wei, H.W. Hou, L.K. Li, Y.T. Fan, Y. Zhu. *Cryst. Growth Des.*, **5**, 1405 (2005).
[29] S.R. Fan, L.G. Zhu. *Inorg. Chem.*, **46**, 6785 (2007).
[30] A. Pellissier, Y. Bretonniere, N. Chatterton, J. Pecaut, P. Delangle, M. Mazzanti. *Inorg. Chem.*, **46**, 3714 (2007).
[31] S. Natarajan, J.K. Sundar, S. Athimoolam, B.R. Srinivasan. *J. Coord. Chem.*, **64**, 2274 (2011).
[32] D.L. Reger, C.A. Little, M.D. Smith. *Inorg. Chem.*, **41**, 19 (2002).
[33] Y.Z. Shen, J.L. Han, T. Rüffer, C.X. Du, Y. Pan. *Inorg. Chim. Acta*, **357**, 2205 (2004).
[34] X.L. Wang, Y.Q. Chen, Q. Gao, H.Y. Lin, G.C. Liu, J.X. Zhang, A.X. Tian. *Cryst. Growth Des.*, **10**, 2174 (2010).
[35] K. Chen, Z.G. Sun, Y.Y. Zhu, Z.M. Liu, F. Tong, D.P. Dong, J. Li. *Cryst. Growth Des.*, **11**, 4623 (2011).
[36] Q.Y. Li, F. Zhou, C. Zhai, L. Shen, X.Y. Tang, J. Yang, G.W. Yang, Z.F. Miao, J.N. Jin, W. Shen. *Inorg. Chem. Commun.*, **14**, 843 (2011).